Hydrogeology Journal (2022) 30:1349–1366
https://doi.org/10.1007/s10040-022-02487-4

REPORT

Reconnaissance of the Diquini and Mariani springs and insights regarding the Massif de la Selle karst aquifer of Haiti

Wm Javan Miner[1] · **James K. Adamson**[1] · **Pierre-Yves Rochat**[2]

Received: 10 June 2021 / Accepted: 27 April 2022 / Published online: 8 June 2022

Abstract

A reconnaissance was performed for Tunnel Diquini and Source Mariani in the metropolitan region of Port-au-Prince, Haiti, to address concerns of decreasing flows and to evaluate potential impacts of a proposed river diversion scheme in the study area. The tunnel and spring are the two largest water sources serving the Port-au-Prince municipal water system and discharge from the Massif de la Selle carbonate aquifer. Considering their significance and importance to the water security of the region, there are limited data or studies specific to the water sources. An introductory framework was established regarding the flow regimes, the origin of waters, and recharge dynamics of the sources. Field reconnaissance and stable-isotope, tracer, and chloride-mass-balance techniques were applied to strengthen the conceptual understanding of the water sources. Recharge to this portion of the Massif de la Selle carbonate aquifer is variable depending on monthly rainfall intensity and 3–7-year climatic cycles. Rather than a consistent long-term decreasing flow trend, a particularly intense period from 2007 through 2010 resulted in the highest flows on record, which have steadily recessed to historical norms in recent years. The recharge characteristics and catchment areas indicate that neither water source is connected to the River Momance; however, a connection to the River Froide is possible, particularly related to the tunnel. Finally, recharge rates and an estimate of renewable groundwater in the Massif de la Selle show the regional significance and importance of the carbonate aquifer for current supplies and future water development.

Keywords Haiti · Karst · Springs · Groundwater/surface-water relations · Groundwater recharge

Introduction

Karst carbonate rocks cover approximately 15% of Earth's ice-free land surface and such aquifers supply ~10% of the world's drinking water (Goldscheider et al. 2020; Stevanovic 2019). Ford and Williams (2007) estimate that at least 25% of the global population partly relies on carbonate aquifer systems. Springs discharging from these aquifers support critical domestic and agricultural water demands and also have significant ecological, cultural, historical and recreational value (Goldscheider 2019). Some of the world's largest cities, including Rome (Italy), Vienna (Austria), Damascus (Syria), and San Antonio (Texas, USA), rely on karst aquifers and springs, supported with significant investment, research, monitoring and protection for the resource (Plan and Stadler 2010; La Vigna et al. 2016; Smiatek et al. 2013; Tian et al. 2021).

The island of Hispaniola, comprising the Dominican Republic and Haiti, includes the two largest cities in the Caribbean—Santo Domingo and Port-au-Prince, respectively—both of which are partly reliant on karst aquifers with transboundary extents in the mountains and plains (Adamson et al. 2016). The regional metropolitan area of Port-au-Prince (RMPP) has a population of 2.8 million which is expected to increase to 3.5 million by 2030 (CIA 2020); the region is rapidly urbanizing and water demand exceeds supply (Adamson et al. 2022, this issue). RMPP is indeed another major city that is significantly reliant on karst springs—approximately 65% of the municipal supply originates from 15 springs and two tunnels that discharge from the Massif de la Selle carbonate aquifer system. The

This article is part of the topical collection "Advancements in hydrogeological knowledge of Haiti for recovery and development"

✉ Wm Javan Miner
javan@northwaterco.com

[1] Northwater International, 2 Bolin Heights, Suite D, Chapel Hill, NC 27514, USA

[2] Rezodlo, S.A., Petion-ville, Haiti

two largest sources are Tunnel Diquini (Diquini) and Source Mariani (Mariani), which combine to source ~42% of the total municipal production. Diquini is a bedrock tunnel and the city's largest water source, while Mariani is the largest naturally flowing spring that supplies the system and it is the most distal source from Port-au-Prince.

Diquini and Mariani have been scarcely researched and studied considering their significance, national importance, and their role as the primary water source of the Port-au-Prince area. Adamson et al. (2022) discuss the regional significance and recharge related to the regional aquifer system and Gonfiantini and Simonot (1988) present discrete isotopic and hydrochemistry data that include springs from the aquifer. Apart from sporadic discrete flow and water quality data over the last several decades, the Centre Technique d'Exploitation de la Region Metropolitaine de Port-au-Prince (CTE-RMPP) was unaware of any historical data or commissioned studies.

Data scarcity related to the springs inhibits the efficient and timely application of science and research to inform planning and investments to improve water security. Spring hydrology has arisen as a major concern for the Government of Haiti and international financial institutions (IFIs). The hydrology and origin of flows are poorly understood and discharge rates are difficult to forecast, thus have arisen as a significant vulnerability to water security and resiliency, especially as water demand exceeds supply and the nation faces climate change impacts (CIAT 2013). Perceptions of decreasing flows over the last decade have been broadly attributed to deforestation, climate change, and the earthquake on 12 January 2010 (Mw = 7.0), however unsupported by data and research. Furthermore, inquiries have been recently raised by IFIs about possible hydrological impacts to the springs from dam and diversion infrastructure under consideration for rivers dissecting the Massif de la Selle. This study is part of a coordinated effort by the Government of Haiti and IFIs to understand the hydrology, origin and connection to surface-water resources of Diquini and Mariani in order to guide water resource planning for RMPP.

Study area

Context and setting

Haiti is experiencing population growth, urbanization, climate change impacts and subsequent increasing water demands. This is particularly true in the RMPP where approximately 23% of Haiti's population resides (United Nations 2019) and water demands are estimated in the range of 365,000 m^3/day (Agbar 2013; E. Moliere, CTE-RMPP, personal communication, 2018). The current water infrastructure capacity is in the range of 100,000–200,000 m^3/day (unpublished water supply production volumes, provided by Pierre Colon Geffrard, CTE-RMPP, 2019, hereafter referred to as "CTE-RMPP, unpublished data 2019").

The study area is located ~10 km WSW of Port-au-Prince, the capital city of Haiti, in the Ouest Department. The area consists of the Massif de la Selle mountain range and the foothills along its northern flank which are bounded to the north by the Baie de Port-au-Prince (Fig. 1), while the Plaine de Leogane lies to the west and the Plaine du Cul-de-Sac is to the east. Topography varies from sea level along the coast to over 1,700 meters above sea level (masl) in the mountains. The mountainous terrain is deeply dissected by the E–W trending Enriquillo-Plaintain-Garden Fault Zone (EPGFZ). The River Froide (R. Froide) and River Momance (R. Momance) are two river systems that flow in the EPGFZ before each is diverted northward, the R. Froide at Carrefour and R. Momance at Leogane (Fig. 1).

Land cover in the northern portion of the study area, including the areas around the tunnel and spring outlets, is moderate to high density residential and commercial with some light industry. Southward into the foothills and Massif de la Selle there is a sharp transition to subsistence agriculture, scrublands, charcoal cultivation, and dispersed vegetation. Woodring et al. (1924) described the watershed above Diquini as primarily scrub vegetation, indicating perhaps that land cover has not changed considerably in this watershed over the last 100 years.

Tunnel Diquini

Tunnel Diquini was completed in 1940 by the J.G. White Engineering Corporation. The tunnel portal is located at 18.5168 N, 72.3929 W at an elevation of 140 masl (Fig. 1). Study, design, and construction documents for the tunnel were not available. It is believed that the tunnel targets an E–W trending normal fault in Eocene-age limestone approximately 1.5 km south of the portal. North of the fault, additional flow enters the tunnel from sidewall and roof seeps along fractures, merging with the main channel flowing toward the portal (Fig. 2). Average annual discharge from the tunnel is estimated at 10.8 Mm^3/year.

Source Mariani

The spring captage is located at 18.5352 N, 72.4269 W at an elevation of 24 masl (Fig. 1). The spring discharges from Eocene-age limestones which drain a portion of the Massif de la Selle carbonate aquifer system west of the R. Froide and north of the R. Momance. A spring protection area of ~4.5 ha has been fenced and reforested. The captage is a broad concrete structure with block perforations to allow inflow from the colluvial deposits, which transmits

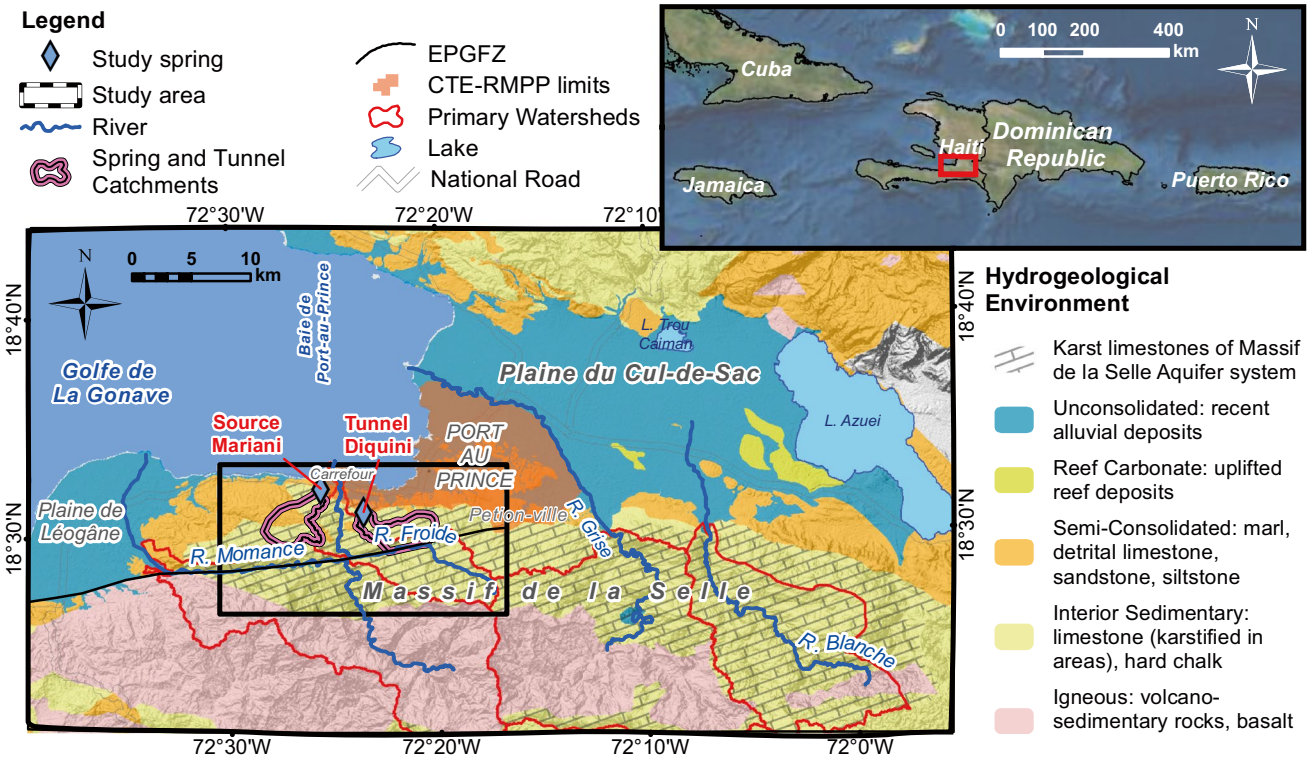

Fig. 1 Map of the study area, hydrogeological environments, major hydrologic features and urban extent

the groundwater to the surface (Fig. 2). Average annual discharge from Mariani is estimated at 7.1 Mm^3/year.

Climate

The study area ranges from semiarid near the coast to semi-humid or humid in the southern mountains (FAO 2010). Average annual rainfall ranges from 1060 mm/year near the coast to over 1,700 mm/year in the upper reaches of the R. Froide basin (Fick and Hijmans 2017). Based on data from the Petion-ville meteorological station of Unité Hydrométéorologique D'Haïti (UHM, unpublished monthly precipitation data, 2019) and two short-term stations in the Massif de la Selle (BRGM 1990), two distinct rainy seasons occur in the catchment, the first peaking in May and the second peaking in September/October—Fig. 3 and Table S1 of the electronic supplementary material (ESM). Precipitation and weather trends are variable, exhibiting periods of intense rainfall, tropical storms, and hurricanes spaced between periods of relative drought. These 3–7-year cycles appear linked to El Niño and La Niña Southern Oscillation (ENSO) events. A slight increasing trend in annual precipitation is apparent in data from 1960 to 2016 for the Petion-ville station (Fig. 3; UHM, unpublished data, 2019) and is also apparent in WorldClim2 precipitation modeling from 1970 to 2000 (Fick and Hijmans 2017). Analysis of monthly rainfall indicates an increasing frequency of months with precipitation greater than 250 mm, and conversely fewer months with precipitation less than 50 mm (Fig. 3). Anomalous high rainfall and intense hurricane seasons between 2007 and 2010 were followed by decreased precipitation from 2011 to 2015.

Geology

Various researchers have mapped portions of the Massif de la Selle and RMPP geology (Boisson and Pubellier 1987; Cox et al. 2011; Eptisa 2016; Kocel et al. 2016; Pubellier 2000; UNDP 1990). These efforts were synthesized into a geologic map (Fig. 4) and lithologic descriptions (Table 1) with modifications based on field observations. The geology of the study area is comprised of folded and faulted carbonates that range from early Miocene to Paleocene age. In the area surrounding Mariani and north of the Diquini portal, early Miocene (Mi) to late Eocene (Eml) detrital and chalky limestones that have low permeability are prominent (Fig. 5c). A small outcrop at Mariani and a majority of the Diquini adit consist of late to middle Eocene (Ems) hard limestones with thin to massive bedding (Fig. 2a,b). In the area of the tunnel portal, the attitude of limestone bedding is near horizontal (Fig. 2b).

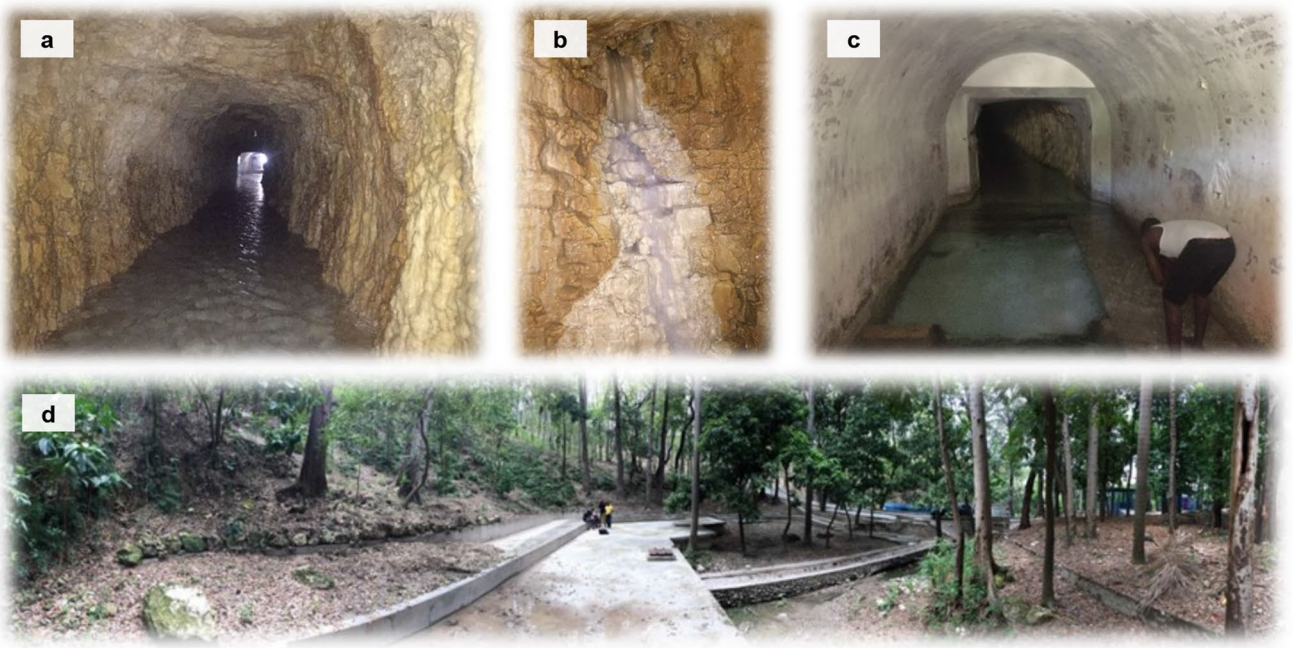

Fig. 2 **a** View of main tunnel adit, **b** example of seep in east tunnel wall, **c** portal of Tunnel Diquini, **d** panoramic view of Source Mariani captage

The entire length of the tunnel is within a hanging wall fault block. The northern wall is down-thrown and may impound groundwater, encouraging flow along the fault through limestone of greater permeability. This fault is believed to be the main source of groundwater feeding the tunnel.

An outcrop of harder limestone at Mariani indicates that the spring exists at the topographic intersection or window with the piezometric surface of the Massif de la Selle aquifer system, recharged farther to the south. The area is otherwise overlain with less permeable rocks. Mariani is the lowest elevation subaerial outlet known for the Massif de la Selle aquifer system. The geologic and topographic intersection may be a key explanation for the consistently high flow rates of the spring, which is effectively a 'drain' for a large portion of the aquifer. Extensive portions of Massif de la Selle appear to be altered by a high degree of karst weathering at elevations above 400 masl based on analysis of LiDAR elevation data (CNIGS 2017). These karst features promote high infiltration and recharge rates within the Eocene limestones that comprise the Massif de la Selle aquifer system.

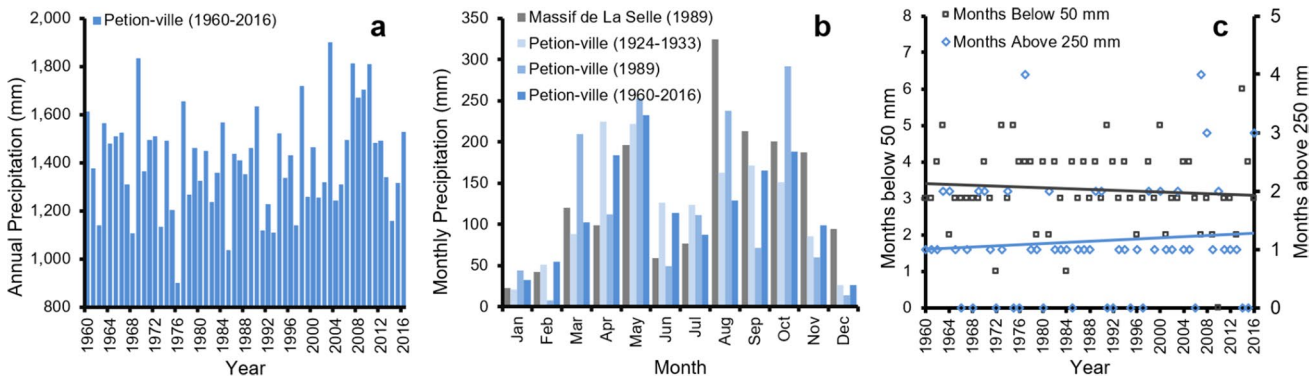

Fig. 3 **a** Total annual precipitation at Petion-ville station from 1960–2016, **b** average monthly precipitation at Petion-ville and Massif de la Selle in 1989 (BRGM 1990), 1924–1933 and 1960–2016 periods (UHM, unpublished data, 2019) and **c** months with precipitation above 250 mm/month or below 50 mm/month at Petion-ville station (UHM, unpublished data, 2019)

Methods

Data collection

Several brief field visits to Diquini and Mariani were conducted to collect samples, inspect local geology, and measure flow rates; Diquini was visited on 15 April 2018 and Mariani was visited on 12 April 2019 and 16 January 2020. Diquini and Mariani discharge measurements were compiled from historical reports and a database (DGTP 1918–1938; Eptisa 2016; Waite 1960). Manually documented readings from totalizing flow meters (Mariani) and a staff gauge (Diquini) were found by CTE-RMPP and were reviewed and digitized for plotting and analysis. Instantaneous flow measurements during the site visits were measured using a top-set wading rod and Marsh-McBirney Flo-Mate 2000 portable electromagnetic velocity meter.

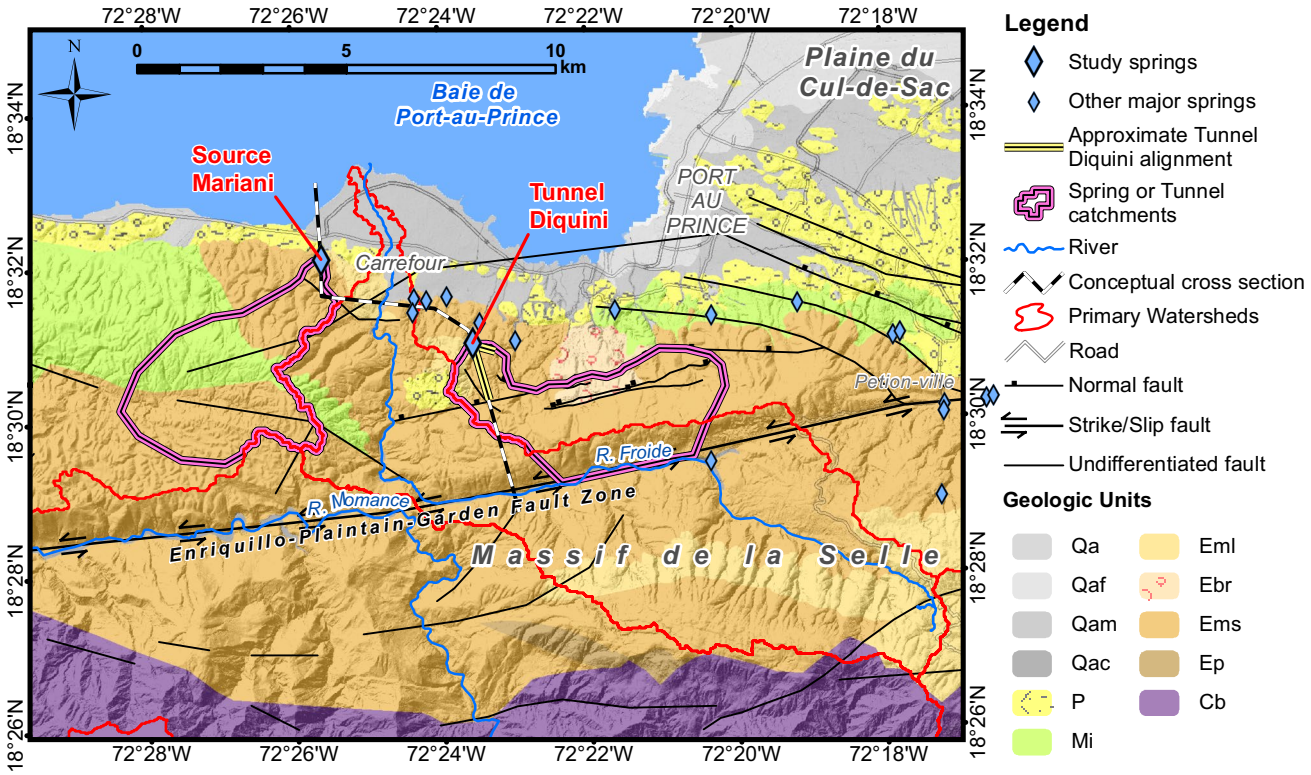

Fig. 4 Geologic map of the study area and major hydrologic features (modified from Boisson and Pubellier 1987; Cox et al. 2011; Eptisa 2015; Pubellier 2000; UNDP 1990). See Table 1 for descriptions of geologic units.

Table 1 Primary geologic units in the study area (modified from Boisson and Pubellier 1987; Cox et al. 2011; Eptisa 2016; Kocel et al. 2016; Pubellier 2000; UNDP 1990)

Code	Age	Description
Qa, Qaf, Qam, Qac	Quaternary	Recent alluvial deposits: (Qa) undifferentiated; (Qaf) fine-grained; (Qam) medium-grained, associated with deltaic fan deposits; (Qac) coarse-grained, associated with river channels
P	Pleistocene	Semiconsolidated colluvial and alluvial deposits of sand, gravel and occasional uplifted reef deposit
Mi	Lower Miocene	Detrital limestone, sandstone and marl
Eml	Upper Eocene	Marl and detrital limestone
Ebr	Upper Eocene	Brecciated limestone
Ems	Middle to Upper Eocene	Hard limestone, often karstified
Ep	Lower Eocene to Paleocene	Limestone and conglomerate
Cb	Cretaceous	Basalt

Data mining uncovered electrical conductivity (EC), pH, turbidity, temperature, chloride and nitrate water quality data for the Diquini and Mariani features (CTE-RMPP, unpublished data 2019; Eptisa 2016) from 2006 through 2015 and 2008 through 2016, respectively. As part of reconnaissance activities, a 12V sampling pump with flexible tygon tubing was used to collect low-flow samples from laminar tunnel flows at Diquini and from inside the spring captage at Mariani. Field water quality was measured using an Oakton PCSTestr for pH, temperature, and EC. Laboratory analysis of major ions, physical parameters, and metals was performed by First Environmental Laboratories in Naperville, Illinois, USA, and ENCO Laboratories in Cary, North Carolina, USA. Stable isotopes in water ($\delta^{18}O$ and δD) were analyzed by Isotech Laboratories in Champaign, Illinois, USA. Chlorofluorocarbon (CFC) and sulfur hexafluoride (SF6) samples were collected in laboratory-provided bottles and copper tubes and analyzed by the University of Utah Noble Gas Lab in Salt Lake City, Utah, USA. Sampling followed methods described by the US Geological Survey, the Reston Chlorofluorocarbon Laboratory, and the University of Utah Noble Gas Laboratory. Precipitation samples were collected opportunistically between 2016 and 2019 and analyzed for chloride. These samples were all collected from the Massif de la Selle in the vicinity of the study area at elevations ranging from 380 to 1,025 masl.

Chloride mass balance

Groundwater recharge to Diquini and Mariani was estimated using chloride mass balance (CMB) methods. CMB has been widely used to estimate groundwater recharge rates (Crosbie et al. 2018; Jebreen e al. 2018; Marei et al. 2010; Naranjo et al. 2015; Troester and Turvey 2004; Ting et al. 1998). In its simplest form, a CMB is calculated via Eq. (1):

$$R = P \times \frac{Cl_p}{Cl_{gw}} \tag{1}$$

where R is recharge (mm/year), P is precipitation (mm/year), Cl_p is average chloride concentration in precipitation across the recharge area and Cl_{gw} is the average chloride concentration in groundwater.

Several assumptions are made in the CMB analysis including: (1) no leaching or adsorption occurs within the aquifers, (2) groundwater depths limit evaporation, (3) surface runoff is limited, and (4) the absence of additional chloride sources like road salt, wastewater, or fertilizer (Marei et al. 2010). The mountainous karst topography, deep water tables, and semihumid climate of the study area satisfy assumptions 1 and 2. Surface drainage features are poorly developed in the hills south of Diquini and Mariani, with abundant sinks and karst features indicating that surface runoff is low (assumption 3). This is further supported by the limited flashiness of R. Froide hydrology compared to other rivers in the region.

Additional sources of chloride are likely limited to wastewater as there is no road salt application and only subsidence agriculture in the probable catchments where fertilizer application is uncommon. Wastewater from latrines or septic systems is considered the primary potential source of chloride contamination; however, robust methods of assessing this impact such as Cl/Br ratio (Marei et al. 2010; Katz et al. 2011; Xanke et al. 2020) were not applicable due to the limited data available. Geographic information system (GIS) analysis (Fig. 6) indicates that primary sources of wastewater chloride are limited in the probable catchment areas as population density is low and there are no or limited piped water systems upgradient of Diquini or Mariani. There is denser urbanization in the area immediately upgradient of Mariani; however, lower permeability strata overlying the limestone significantly reduce contamination susceptibility.

Fig. 5 **a** Example outcrop of middle to upper Eocene age (Ems) hard, micritic and well-bedded limestone, **b** example of near horizontal bedding in tunnel limestone, **c** example outcrop of lower Miocene to upper Eoecene (Mi, Eml) detrital limestone, chalk and marl

Mariani and Diquini were further evaluated for wastewater-origin chloride, with available nitrate and turbidity data compared to chloride, discharge, and EC (Fig. 7a–d). Karst spring water subjected to wastewater contamination typically exhibit a positive correlation between chloride and nitrate (Xanke et al. 2020) and a negative correlation when contamination is limited (Shamsi et al. 2019). Diquini waters appear to be exposed to little to no contamination, while Mariani waters may have slightly higher contamination (Fig. 9a). Both sources have similar average nitrate concentrations of 10.1 and 12.5 mg/L NO_3–N, respectively, exhibiting limited variability with flows (Fig. 9b). Mariani waters show significantly higher pulses of turbidity, which is poorly correlated to either the EC (Fig. 9c) or discharge rate (Fig. 9d).

Numerous studies have presented nitrate data for karst springs with varying levels of wastewater contamination (Table 2). Both Diquini and Mariani waters have nitrate concentrations in the low/potentially increasing contamination range. Springs considered contaminated and requiring chloride correction for CMB analysis have nitrate concentrations at least twice as high as Diquini and Mariani. As a result of these justifications, the CMB approach for estimating recharge rates can be reasonably considered as a first step in evaluating the karst catchments. CMB results should be applied with caution, however, due to data limitations. Further data collection of Diquini, Mariani, and rainfall will support the refinement of CMB estimates and catchment analysis.

Catchment delineation

Catchment areas were estimated using a combination of methods. First, the catchment size (area) was estimated based on the recharge rates from the CMB, annual average discharge, and variable annual precipitation based on altitude (Fick and Hijmans 2017). The stable isotope altitude effect was applied to estimate the minimum and mean recharge elevations in a manner similar to other researchers (Gonfiantini and Simonot 1988; Luo et al. 2018; Matheswaran et al. 2019; Yehdegho and Reichl 2002). Lastly, remote sensing and topography data were interpreted to delineate possible catchment extents based on the mean recharge altitude of the isotope analysis, and the catchment area estimates from CMB and flow analysis. For Diquini, the catchment extent was also guided by the mapped extent of the normal fault that the tunnel reportedly targeted and intersected.

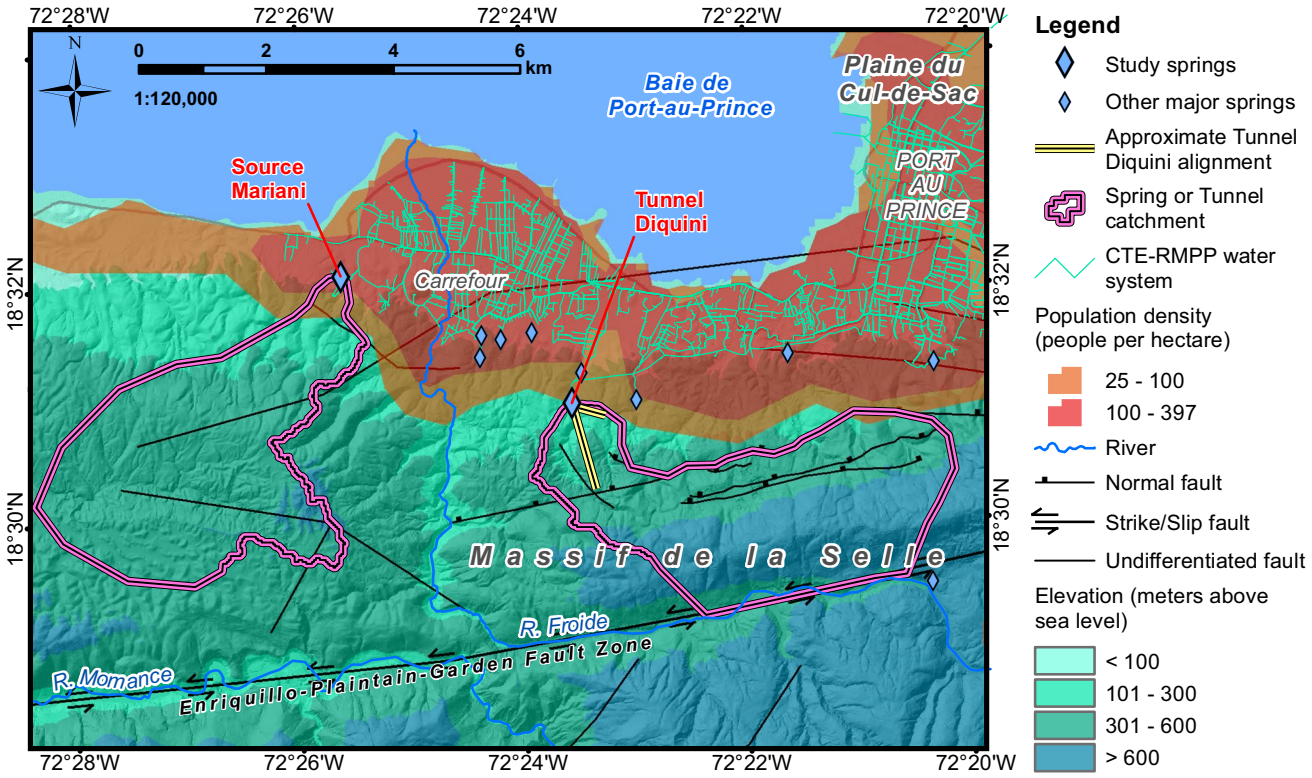

Fig. 6 Elevation and catchment areas relative to CTE-RMPP water system and dense urban areas

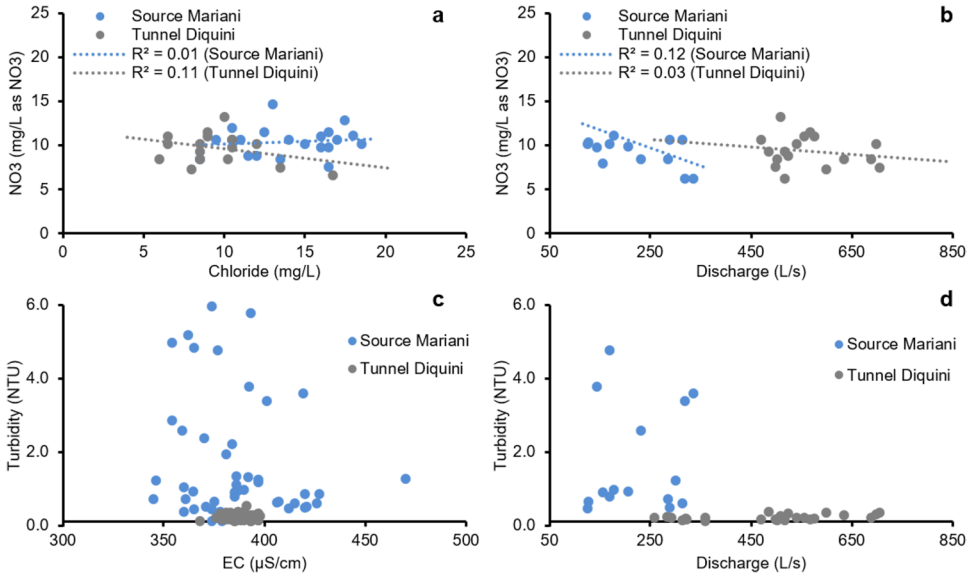

Fig. 7 Discharged waters from Diquini and Mariani: **a** chloride compared to nitrate, **b** discharge compared to nitrate, **c** electrical conductivity (EC) compared to turbidity, and **d** discharge compared to turbidity

Results

Discharge

Both Diquini and Mariani display similar discharge characteristics, with a coefficient of variation between 0.33 (Diquini) and 0.31 (Mariani) and 90th percentile flows approximately 2.3 times larger than 10th percentile flows. The average flow of Diquini is ~1.5 times greater than Mariani (Table 3; Table S2 of the ESM).

Diquini and Mariani discharge plotted versus contemporary annual precipitation and prior year precipitation shows that Diquini discharge is highly correlated to prior year precipitation, while Mariani discharge is equally correlated to prior and contemporary precipitation (Fig. 8a,b). Similar lag correlations between prior year precipitation and spring or river discharge have been noted by researchers in Belize (Tennielle Williams, Belize National Hydrological Services, personal communications 2021), Australia (Anderson et al. 2019), Italy (Fiorillo et al. 2021), and Slovakia (Malík et al. 2021).

Diquini flow exhibits stronger correlation than Mariani to the number of months in the prior year with precipitation greater than 250 mm; a clear trend is apparent as more months exceeding this value correlated to higher and more reliable tunnel flows in the subsequent year. Jones and Banner (2003) reported similar findings with a monthly threshold of 190–200 mm/month for karst recharge in Barbados, Guam, and Puerto Rico. Baker et al. (2020) noted a higher threshold of 76–79 mm/week in a subtropical karst terrain in Australia. The differences between Diquini and Mariani may be related to the elevation of the discharge outlets, Diquini

Table 2 Values of groundwater nitrate in various karst springs

Study	Area	Degree of contamination (mg/L as NO_3)[a]		
		Moderate/high	Increasing	Low
Amiel et al. (2010)	Jerusalem, Israel	83–117	-	-
Kamps et al. (2009)	Texas, USA	-	-	6.6–7.3
Kang et al. (2011)	Shandong, China	43	-	~10
Long et al. (2008)	South Dakota, USA	-	-	0.4–1.8
He et al. (2010)	Chongquing, China	22–48	-	-
Huang et al. (2019)	Yunan, China	-	5.4–10.6	-
Xanke et al. (2020)	Lower Jordan Valley, Jordan	58.1	-	
Shamsi et al. (2019)	Mazandran, Iran	-		4.4–9.2
Luo et al. (2018)	Hubei, China	-	7.4–23.8	-
Yehdegho and Reichl (2002)	Switzerland	-	-	2.6–6.7
Mudarra et al. (2014)	Andalusia, Spain	-	-	2–5.4

[a]Degree of contamination based on description of researchers for each study

at a higher elevation represents mixed perched and regional groundwater, and Mariani exhibits more well-mixed regional groundwater at a lower elevation.

Hydrochemistry

Diquini and Mariani waters are Ca–HCO_3 type (Fig. 9; Table 4), which is typical of karst limestone aquifers. Both sources are relatively dilute, with average total dissolved solids (TDS) content of 203 and 200 mg/L, respectively (Table S3 of the ESM). Mariani has a higher average chloride concentration (14.4 mg/L) compared to Diquini (9.2 mg/L), which may be indicative of lower recharge rates to Mariani.

Stable isotope and environmental tracer

Diquini and Mariani waters plot very near the local meteoric water line (LMWL; Fig. 10), similar to 29 other springs sampled by Gonfiantini and Simonot 1988), indicating limited exposure to evaporation prior to recharge. They also plot midway between R. Grise and R. Momance, displaying a strong E–W stable isotope gradient.

Based on CFC and SF6 tracer results (Table 5), both Diquini and Mariani waters have an average estimated age of 30 years. Stable isotope values are similar to results from the 1980s (Gonfiantini and Simonot 1988), indicating that the outflows originate from the well-mixed regional Massif de la Selle aquifer system, and perhaps limited changes to the hydrological regime have occurred over the past 40 years. Such consistency further suggests that changes in precipitation patterns may be a primary driver of discharge variation through time.

Table 3 Summary discharge (Q) statistics for Diquini and Mariani

Flow statistic	Tunnel Diquini (L/s)	Source Mariani (L/s)
Average, arithmetic (Q)	341	225
Standard deviation (Q_{SD})	112	70
Coefficient of variation (CV)	0.33	0.31
Maximum (Q_{max})	848	355
Minimum (Q_{min})	128	88
10th percentile (Q_{10})	212	139
90th percentile (Q_{90})	483	324
Median (Q_{50})	320	221
Count	425	73
Date range	1959, 1980–2018	1925–1933, 2008–2010, 2014–2020

Recharge

The CMB analysis (Table 6; Table S4 of the ESM) indicates high autogenic karst recharge in the Massif de la Selle within both Diquini and Mariani catchments. Recharge to Diquini averages 60%, ranging between 47% in normal precipitation years to 69% in high precipitation years. Mariani averages 38%, ranging between 33 and 49%. Further discussion of these recharge estimates is provided in subsequent sections.

Catchment areas

Based on the CMB, precipitation and discharge data, Diquini and Mariani are estimated to have approximately 12.4 and 13.3 km^2 recharge catchments, respectively. The Diquini and Mariani catchments have minimum and average recharge elevations of 200–650 masl and 100–580 masl, respectively, based on the stable isotope altitude relationship developed by Gonfiantini and Simonot (1988) shown in Fig. 11 relative to Diquini,

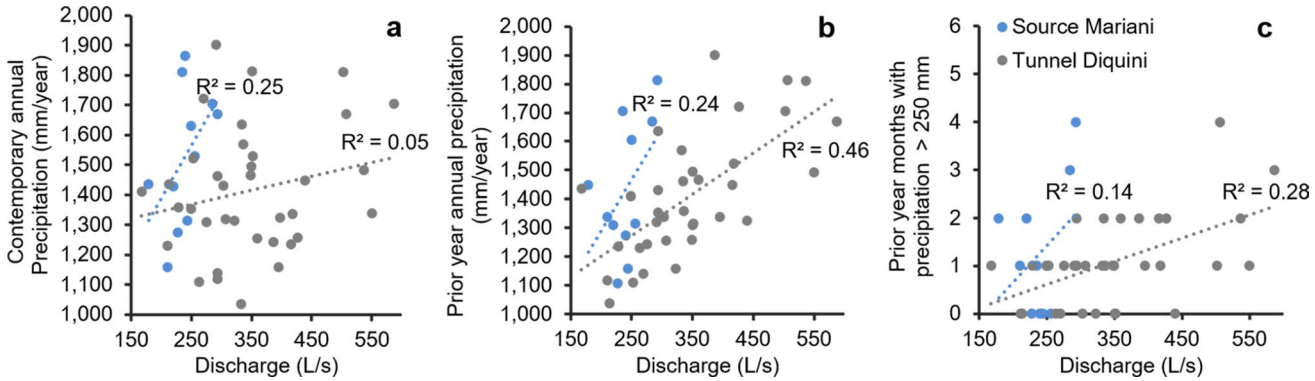

Fig. 8 **a** Diquini and Mariani flow compared to contemporary-year total precipitation, **b** prior-year total precipitation, and **c** prior-year number of months with precipitation greater than 250 mm (CTE-RMPP, unpublished data, 2019; Eptisa 2016; Northwater International and Rezodlo (2018); Northwater International and Rezodlo 2020; UHM, unpublished data for Petion-ville meteorological station, 2019)

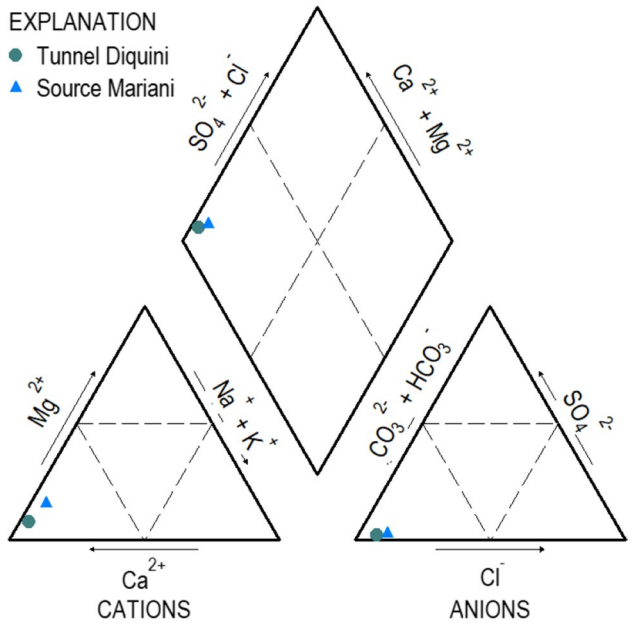

Fig. 9 Piper plot of average Tunnel Diquini and Source Mariani waters

Mariani and other springs. While both sources have similar catchment areas, variability in recharge rates suggests that aerial recharge for Diquini may be as high as 0.875 Mm^3/km^2 and on the order of 0.533 Mm^3/km^2 for Mariani. Preliminary catchment area interpretations are shown in Figs. 1, 4 and 6. Further research and data collection is necessary to more accurately delineate these catchments.

Discussion

Conceptual groundwater origin and flow

A conceptual hydrogeologic cross section illustrates the apparent groundwater origin and flow to Diquini and Mariani (Fig. 12). Diquini derives its flow from intersecting perched karst systems and well-mixed regional groundwater predominately from a fault system. Mariani acts as a low-elevation 'drain' of the Massif de la Selle aquifer. This results in the greater fluctuations in flow at Diquini relative to the more stable flows at Mariani.

The catchment of Diquini extends eastward along the mapped normal fault, but also southward to the EPGFZ and a channel of the R. Froide. Conversely, the Mariani catchment does not likely extend southward into the R. Momance watershed. This factor and topographic analysis may indicate that streamflow losses in the upper reach of R. Froide could be a source of recharge to the portion of the aquifer which supplies Diquini.

Groundwater recharge dynamics

Analysis of the long-term hydrograph for Diquini and Mariani relative to major climatic events (Fig. 13) provides important insights into recharge dynamics. First, groundwater recharge in the portion of the Massif de la Selle carbonate aquifer appears to vary significantly by climatic cycles. These cycles appear to correspond to El Niño and La Niña Southern Oscillation (ENSO) events (occurring on 3–7-year cycles) and their associated increases or decreases in precipitation. The data from 1980 to 2000 display these cycles clearly, with high rainfall years, such as 1984, 1990, 1994, and 1998, leading to large increases in Diquini discharge while flow recession is apparent during low and even normal rainfall years. Similar trends have been noted related to ENSO in Haiti (Moknatian and Piasecki 2021) and Nicaragua (Adamson et al. 2021) or other climatic trends in Cuba (Fernández-Alvarez et al. 2020), Italy (Fiorillo et al. 2021) and Australia (Anderson et al. 2019). Furthermore, based on the CMB, both Diquini and Mariani catchments appear to receive ~30% more recharge during high precipitation cycles (2007–2010) than in normal or lower precipitation periods (2011–2019). This corroborates with the increased flow rates after these high precipitation periods (Fig. 13) and with increased flow rates after years with a greater proportion of months with precipitation greater than 250 mm (Fig. 8).

Second, since 2000, this trend has been somewhat masked by the intense rainfall years of 2007 through 2010 when several devastating storms occurred during a La Niña period.

Table 4 Average groundwater major ion concentrations (CTE-RMPP, unpublished data 2019; Eptisa 2016; Northwater International and Rezodlo 2018, 2020)

Source	Calcium (mg/L)	Magnesium (mg/L)	Sodium (mg/L)	Potassium (mg/L)	Carbonate (mg/L)	Bicarbonate ($CaCO_3$) (mg/L)	Chloride (mg/L)	Sulfate (mg/L)	TDS (mg/L)
Tunnel Diquini	76.5	4.0	2.8	0.70	0.0	256	9.2	4.5	200.2
Source Mariani	79.3	9.6	6.3	1.07	0.0	240	14.4	6.1	203

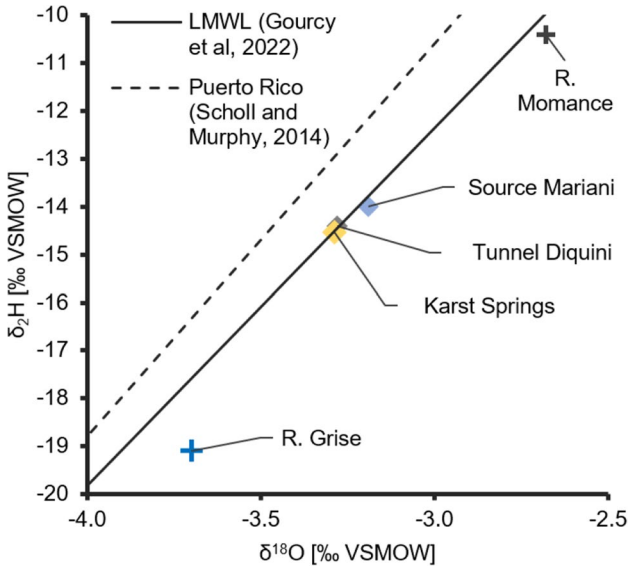

Fig. 10 Tunnel Diquini and Source Mariani samples plotted relative to the local meteoric water line (LMWL) and nearby major groundwater and surface-water resources. Sources: Gourcy et al. (2022, this issue), Scholl and Murphy (2014)

These coupled years of extreme rainfall resulted in the highest sustained flows on record during a period in which increased attention was focused on Haiti and the RMPP area in particular due to the 12 January 2010 earthquake (Mw = 7.0). Since 2010, flows have generally recessed back toward the long-term average, which appears as a decadal decrease in flow. The importance of these tropical storms has been noted by other researchers in the Caribbean (Fernández-Alvarez et al. 2020; Stallard and Murphy 2012).

Third, the discharge rates of Mariani have not increased as dramatically during the 2007–2010 period relative to 2014 and onward, which highlights different recharge dynamics between the two sources. Diquini discharges a greater proportion of perched and seasonal groundwater, while Mariani acts more as a pressure relief drain to the lower-elevation portion of the regional aquifer discharging well-mixed waters. This observation correlates to comparisons of prior-year total precipitation and the 250-mm monthly precipitation threshold (Fig. 8); a stronger correlation occurs for Diquini versus Mariani.

Table 6 Summary statistics for chloride in groundwater and Massif de la Selle precipitation (CTE-RMPP, unpublished data, 2019; Eptisa 2016; Northwater International and Rezodlo 2018; Northwater International and Rezodlo 2020) along with calculated recharge rates. Complete chloride datasets available in Table S4 of the ESM. *SD* standard deviation

	Precipitation	Tunnel Diquini		Source Mariani	
	(mg/L)	(mg/L)	(percent)	(mg/L)	(percent)
Average (all)	5.5	9.2	60%	14.4	38%
Average (2008-2010)	NA	8.0	69%	11.2	49%
Average (2011–2019)	NA	11.7	47%	16.7	33%
SD	5.9	3.2	-	3.7	-
Count	12	44	-	29	-

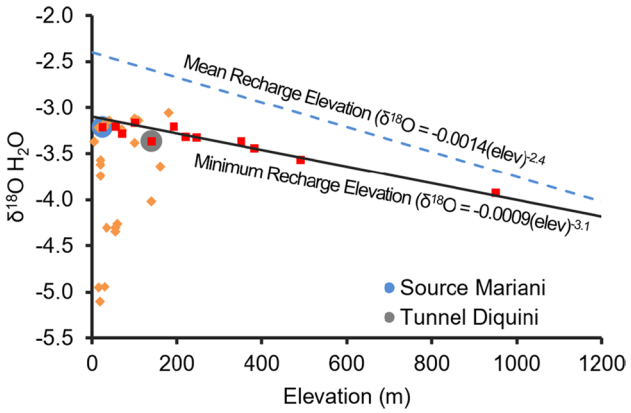

Fig. 11 Various karst springs with estimated minimum and mean recharge elevations

Several observations concerning recharge dynamics can also be elucidated from comparison of Diquini and Mariani chloride over time and by discharge rate (Fig. 14). Both Diquini and Mariani display an annual chloride cycle related to pulses of recharge during the rainy seasons. Diquini displays a relatively strong trend of slowly decreasing chloride (higher recharge) as the discharge rates increase, but as flows fall below ~300 L/s, the chloride values increase more rapidly in a manner similar to the Mariani chloride–discharge curve. Similar chloride–discharge relationships were

Table 5 Stable isotope, CFC and SF6 concentrations with calculated groundwater (GW) age (Northwater International and Rezodlo 2018, 2020)

Source	$\delta^{18}O$	δD	CFC-11	CFC-12	CFC-113	SF6 (corrected)	Excess air	Recharge temperature	CFC GW age	SF6 GW age
	(‰)	(‰)	(pptv)	(pptv)	(pptv)	(pptv)	(mL)	(°C)	(years)	(years)
Tunnel Diquini	-3.3	-14.2	224.1	475.3	45.7	2.96	2.0	NA	32	26
Source Mariani	-3.2	-14.0	NA	NA	38.5	4.19	1.5	22.7	35	21

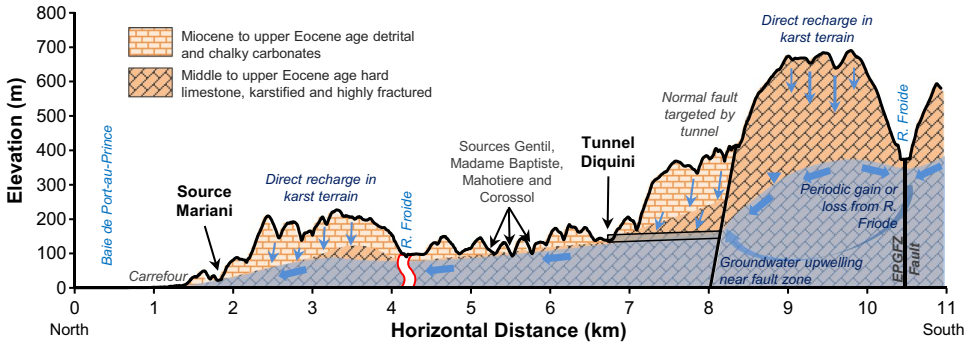

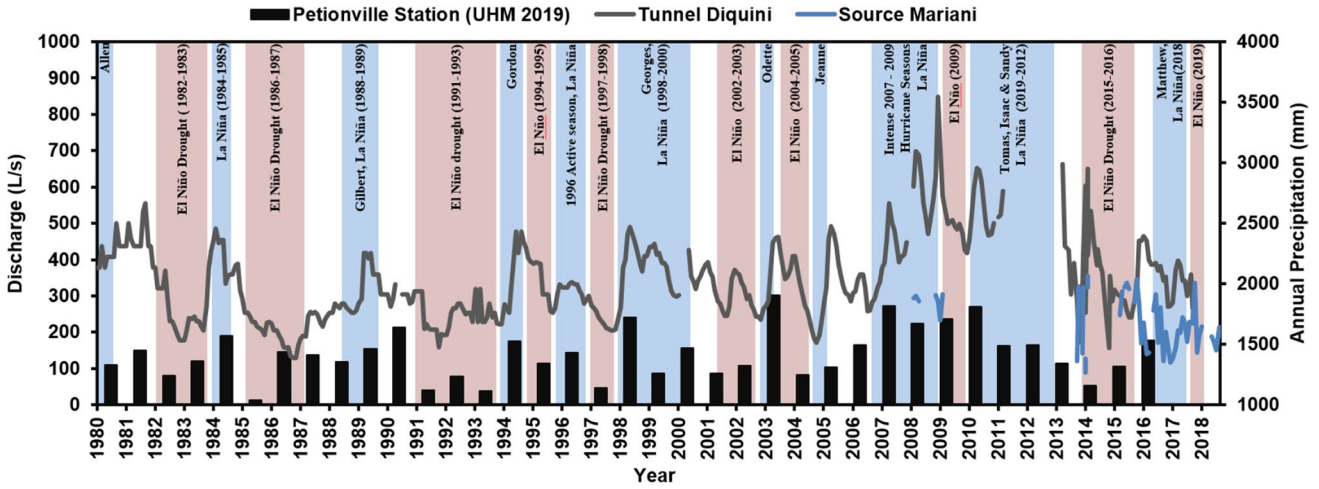

Fig. 12 Generalized hydrogeological cross section of the western Massif de la Selle carbonate aquifer system

Fig. 13 Discharge hydrographs relative to annual average precipitation and climatic cycles

documented by Anderson et al. (2019) in a catchment in Australia. These results suggest that Diquini typically receives around 300 L/s discharge from the regional groundwater flow that also supplies Mariani, and additional seasonal flow of up to an extra 300 L/s from perched groundwater flow.

Recharge rates

The estimated recharge rates suggest rapid infiltration with minimal runoff or evapotranspiration, which is supported by the stable isotope data. While the technique appears applicable to the study area, the results must be applied with considerable caution due to the limited datasets available for analysis. Further study should be focused on refining these estimates, especially concerning precipitation chloride concentrations and spatial/temporal variability in the Massif de la Selle. Independent methods are also necessary to improve recharge study and catchment area delineation.

Rainfall chloride was particularly limited for the CMB; only 12 samples were available with an average value of 5.5 mg/L, which was not weighted to precipitation volumes. Research in other parts of the Caribbean and Central America indicates that this value may be a plausible long-term average rainfall chloride value (Table 7), but also highlights the need for more rainfall data to refine estimates. The most thorough datasets for comparison are from eastern Puerto Rico (Gioda et al. 2013; Stallard and Murphy 2012), which indicate a long-term average annual chloride value of 3 mg/L. Similar values applied to the Massif de la Selle would result in lower recharge rates, and Diquini and Mariani would receive only 32 and 21%, respectively.

However, as described previously, karst terrains typically receive the majority of recharge after a monthly threshold of precipitation has been met, with the highest recharge rates occurring during wet months with storm events (Baker et al. 2020; Jones and Banner 2003). Stallard and Murphy (2012) indicate that depending on the direction, speed, and intensity of tropical storms and hurricanes, the chloride deposition may be several times higher than the long-term average—for example, Hurricane Georges (in 1998) was estimated to result in an average rainfall chloride value of 16.1 mg/L, and the annual chloride deposition for that year was 23% higher

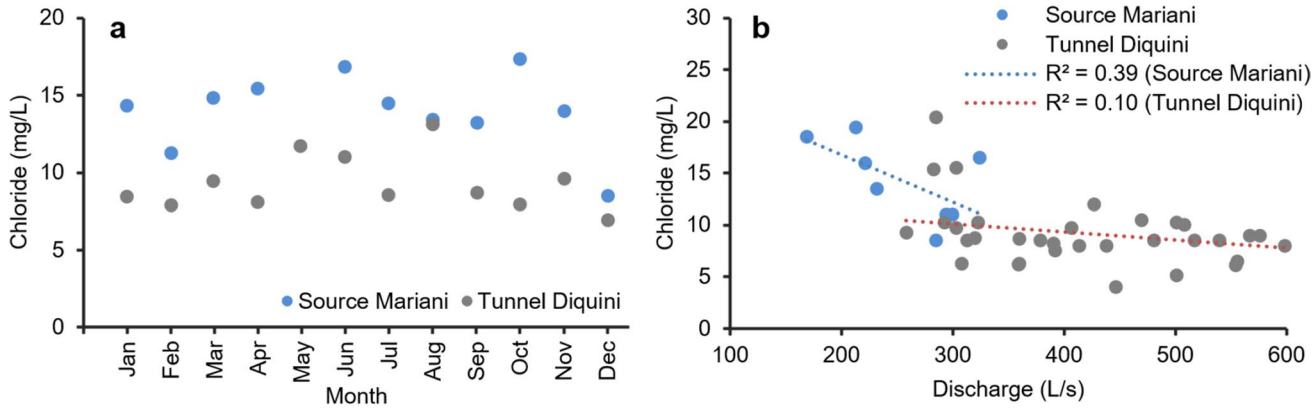

Fig. 14 **a** Monthly average groundwater chloride, **b** Diquini and Mariani flow vs. chloride (CTE-RMPP, unpublished data, 2019; Eptisa 2016; Northwater International and Rezodlo 2018; Northwater International and Rezodlo 2020)

than average. If such concentrations occur during high recharge events in the Massif de la Selle, the estimated CMB recharge rates for Diquini and Mariani may be conservative.

The recharge estimates and supporting data are within the ranges reported by other researchers in the Caribbean and Central America karst terrains. Hartman et al. (2021) performed a global evaluation using available spring discharge rates and soil moisture data, with calibration points in Puerto Rico, to estimate that 50% of karst springs below 1,200-m elevation have recharge rates higher than 45%, with some as high as 70%. Diquini, with an average recharge rate of 60%, is on the high end of estimates in the literature. This is expected, given that it is an anthropogenic or artificial spring that specifically targets a high-permeability fault. Source Mariani, with an average recharge rate of 38%, lies in the mid-range of typically reported karst recharge rates (Table 8), similar to those found in Puerto Rico (Ghasemizadeh et al. 2016) and Florida, USA (Langston et al. 2012).

Groundwater and surface-water interconnection

Understanding the degree and nature of connection between the groundwater and surface-water resources of the Massif de la Selle is a critical component of developing future water supplies for the region, especially as river diversion infrastructure projects are being considered to augment the RMPP water supply. Diquini and Mariani discharge from the same regional carbonate aquifer that provides baseflow to R. Momance, R. Froide, and R. Grise. Understanding how hydrologic changes to the rivers may affect the aquifer was evaluated with stable isotope and recharge area analysis.

River Froide

While data are limited to either confirm or disprove a connection between R. Froide and Diquini or Mariani, the hydrologic dynamics of the three appear linked by the

Table 7 Published precipitation chloride data in Latin America and the Caribbean

Study	Area	Precipitation chloride	
		Range (mg/L)	Average (mg/L)
Pacheco et al. (2004)	E. Cuba	1.8–3	2.1
Corvo et al. (2005)	Havana, Cuba	3.2–45	9.2
Gioda et al. (2013)	E. Puerto Rico	0.82–32	6.1 at elevation 1,051 masl
		0.16–47	4–5.1 at elevation 360–380 masl
		~1 mg/L, less during rainy season	
Adamson et al. (2021)[a]	Nicaragua	2.7–24.3	8.1
Stallard and Murphy (2012)[a]	E. Puerto Rico (1985–2006 Annual)	2.0–4.0	2.8
	E. Puerto Rico (1985–2006 Monthly)	1.6–5.5	3
	E. Puerto Rico (Hurricane Georges, in 1998)[b]	8.9–56	16.1
	E. Puerto Rico (Hurricane Hortense, in 1996)[b]	3.5–9	3.9

[a]Rainfall weighted

[b]Estimated by Stallard and Murphy (2012) based on river runoff

Massif de la Selle carbonate aquifer which lies between the Momance and Grise rivers. The stable isotope trends identified by Gonfiantini and Simonot (1988) indicate that R. Froide baseflow (groundwater) would exhibit a stable isotope composition intermediate to the R. Momance ($\delta^{18}O$ –2.68‰) and R. Grise ($\delta^{18}O$ –3.66‰). Based on the geographic position and mean watershed elevations, R. Froide baseflow $\delta^{18}O$ (between –3.13 and –3.55‰) is estimated. This $\delta^{18}O$ range brackets the values for Diquini and Mariani (–3.3 and –3.2‰, respectively), suggesting that Diquini, Mariani, and R. Froide derive their recharge from the same regional carbonate aquifer system.

As illustrated in Fig. 12, R. Froide traverses the northern edge of the Diquini recharge area at an elevation 150 m higher than the tunnel floor and is nearly 30 m higher in elevation than the Mariani outlet parallel to the hydrogeologic strike just south of Carrefour. The elevated course of the R. Froide, along with the high groundwater gradient implied by groundwater levels at the stream channel surface, suggest the possibility that upper reach streamflow along the EPGFZ could infiltrate to the normal fault and discharge into Diquini. Similarly, lower reach stream losses may infiltrate into the carbonate aquifer contributing to discharge at Mariani. The higher recharge rates for Diquini vs. Mariani may suggest another source of recharge to Diquini, perhaps R. Froide. No noble gas analysis for the Diquini sample was available to estimate recharge temperatures. If streamflow infiltration was significant, the recharge temperature would be higher than otherwise expected due to the warmer surface water.

Both isotope and elevation analyses indicate that there is likely a dynamic hydrogeological relationship between the R. Froide, Diquini, and Mariani. Streamflow monitoring of various reaches, isotopic or tracer monitoring, is necessary to better characterize these relationships.

River Momance

The Diquini and perhaps Mariani catchments appear to overlap with the R. Froide watershed; however, the available data do not suggest that the catchments overlap with the R. Momance watershed located farther inland. This is largely due to the geometry of the EPGFZ that separates the Momance basin. Faults are a primary driver of conduit network development and concentrate recharge laterally (Bauer et al. 2016; Brunetti et al. 2013; Clauzon et al. 2020) as opposed to forming a groundwater barrier, as is typical in lower-permeability clastic sediments (Mayer et al. 2007). The EPGFZ is a major driver of both surface water and groundwater flow in the Massif de la Selle region south of Carrefour. Surface water flow in the R. Momance watershed south of the EPGFZ is diverted westward toward Leogane along the fault, and it is likely that groundwater is similarly diverted. The noble gas analysis conducted along with CFC and SF6 sampling for Mariani indicate a recharge temperature of 22.7 °C (Table 5), which is on the low end of the average temperature in the catchment (23–25 °C). If streamflow infiltration from the R. Momance was a component of recharge to Mariani, the noble gas recharge temperature would be expected to be on the high end of or above the average catchment temperatures.

Long-term trends

The research presented was partly initiated due to concerns that flow rates were on a long-term decreasing trend, which was perhaps accelerated by the 12 January 2010 earthquake. Such long-term trends have been reported in Haiti, specifically within the Massif de la Selle carbonate aquifer (MDE 2001) and other researchers have noted increases in carbonate permeability resulting in temporarily affected discharge after earthquakes (Fiorillo et al. 2021; Nanni et al. 2020; Petitta et al. 2018). The data and analysis presented do not indicate

Table 8 Published karst recharge rates

Study	Area	Karst recharge rate		Method[a]
		(percent)	(mm/year)	
Ghasemizadeh et al. (2016)	Eastern Puerto Rico	9–37	712	MD
Bauer-Gottwein et al. (2011)	Yucatan, Mexico	17–70	500	WB, SD
Andreo et al. (2008)	Southern Spain	17–59	500	WB, GIS
Hartman et al. (2021)	Global	45–70	NA	ST
Malík et al. (2021)	Slovakia	33.5	291	SD
Karami et al. (2016)	Iran	55–70	666	GIS
Langston et al. (2012)	Florida, USA	33–44	450–600	WB
de Vries and Simmers (2002)	Saudi Arabia	47	93	NA
	Algarve, Portugal	27–55	149–303	NA
Jebreen et al. (2018)	Palestine	19–37	111–216	CMB
Mudarra et al. (2014)	Spain	45	342	CMB
Troester and Turvey (2004)	La Gonave, Haiti	4	-	CMB

[a]Methods: *MD* numerical modeling, *WB* water balance, *GIS* geographic spatial analysis, *ST* statistical extrapolation, *SD* spring discharge, *CMB* chloride mass balance, *NA* unknown

an anomalous or alarming long-term decreasing trend of flows from Diquini and Mariani. Discharge rates do vary significantly, as is common in karst systems; discharge variations at decadal to monthly temporal scales are visible in the datasets. Diquini experienced a downward trend in flow rate from 1980 to 1990, a slight upward trend from 1990 to 2000, a strong upward trend from 2000 to 2010, and a decreasing trend from 2010 to 2018. Mariani flows appear to mirror Diquini in the more recent downward trend from 2010 to 2018. Similar decadal trends have been reported by other researchers analyzing long-term spring hydrographs (Fiorillo et al. 2021; Anderson et al. 2019). The more recent trend coincidentally occurs in the shadow of the 2010 earthquake and understandably raised concern about the future flows and water security of the region.

A comparison of discharge rates from both Diquini and Mariani exhibits an increase in average discharge rates, possibly due to the slight increase in months with rainfall in excess of 250 mm—for example, comparing the August 1959 Diquini flow rate (217 L/s) to average August flow rates between 1980 and 2018 (336 L/s) shows an increase which is even more substantial compared to the 2008 to 2018 data (470 L/s). Similarly, for Mariani, comparison between 1925–1933 and recent data suggest remarkably similar average discharge and hint at the possibility of increased flows (Fig. 15). Further study of these long-term and cyclic trends would provide valuable water management and planning insights and may guide further development of the Massif de la Selle aquifer resource.

Insights into the regional Massif de la Selle aquifer

Insights concerning the Massif de la Selle aquifer can be extrapolated from the analysis of the two sources. Using the average recharge rates of Diquini and Mariani (60% or 875 mm/year and 38% or 533 mm/year, respectively) and their potential recharge areas (12.4 and 13.3 km^2, respectively), an average recharge rate of 704 mm/year (0.7 Mm^3/km^2/year) is calculated. This is on the high end but comparable to values found by other researchers in karst terrain, including 0.5 Mm^3/km^2 in Spain (Andreo et al. 2008) and the Yucatan Peninsula in Mexico (Bauer-Gottwein et al. 2011) where rates up to 70% were estimated, and 0.71 Mm^3/km^2 in Puerto Rico (Ghasemizadeh et al. 2016). Extrapolating across the 600 km^2 of the Massif de la Selle carbonate outcrop area equates to 422 Mm^3/year of renewable groundwater. This rate is also comparable to estimates from river baseflow regression techniques (Adamson et al. 2022) which estimated 0.6 Mm^3/km^2/year, or 361 Mm^3/year of recharge, in the R. Grise and R. Blanche portions of the Massif. Scanlon et al. (2002) noted that river baseflow regression provides a minimum recharge rate for a catchment area due to the presence of other surface or subsurface outlets.

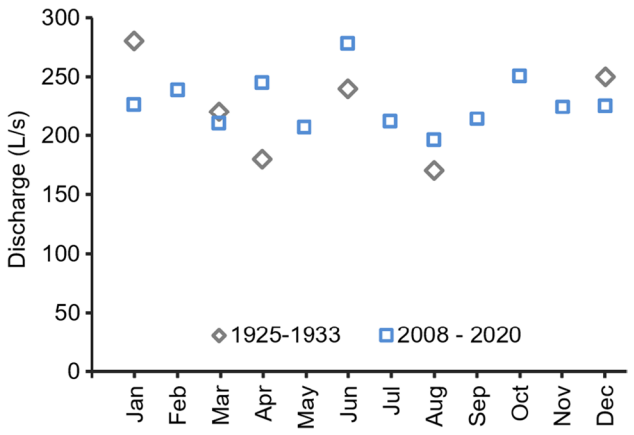

Fig. 15 Comparison of monthly average spring (Source Mariani) discharge through time

Given the consistency of stable isotope values and of groundwater age for Diquini and Mariani waters, a storage estimate was made by multiplying the average annual discharge by average groundwater age (29 years), which results in storage of approximately 312 and 198 Mm^3 for Diquini and Mariani, respectively. Extrapolating this for the entire Massif de la Selle aquifer results in an estimated 10,470 to 12,100 Mm^3 (10.47 to 12.1 km^3) of groundwater storage. For comparison, groundwater modeling of one of Haiti's largest aquifers, the Plaine du Cul-de-Sac, estimated total alluvial storage at 6,320 Mm^3 or 6.32 km^3 (Northwater International and Rezodlo 2019).

The aforementioned discussion points to the significance and importance of the Massif de la Selle carbonate aquifer system in supporting the RMPP and Leogane areas both directly and indirectly. The available recharge of the Massif de la Selle aquifer is likely over 4 times that of the Plaine du Cul-de-Sac and Leogane Plaines combined, while both plains also rely on streamflow infiltration from Massif de la Selle rivers for a majority of their recharge (Adamson et al. 2022). There appears to be potential for further groundwater development of the Massif de la Selle aquifer system; however, further study is needed to reduce some of the uncertainties regarding absolute quantities available and multiannual recharge cycles.

Conclusions

Reconnaissance level sampling has been combined with historical discharge and hydrochemistry data to characterize the two largest single water sources for the Port-au-Prince municipal water system, Tunnel Diquini, and Source Mariani. Key insights concerning discharge characteristics and recharge dynamics were obtained via application of stable isotope, tracer, and chloride mass balance techniques coupled with time-series flow data. Recharge to this portion of the Massif de la Selle carbonate aquifer is highly variable depending on monthly rainfall intensity as well as 3–7-year climatic cycles. A particularly intense period in 2007 through 2010 resulted

in the highest flows on record, which have steadily recessed back to the norm. This insight allays concerns that long-term decreases in flow are occurring at either Diquini or Mariani. The recharge characteristics and catchment areas indicate that neither water source is connected to the R. Momance; however, a connection to the R. Froide may exist, particularly for Diquini. Recharge rates and an estimate of renewable groundwater in the Massif de la Selle have been extrapolated from the Diquini and Mariani data and show the regional significance and importance of the carbonate aquifer for future water development. Insights from this study can be used to guide further characterization of the Massif de la Selle aquifer and water resource development.

Supplementary Information The online version contains supplementary material available at https://doi.org/10.1007/s10040-022-02487-4.

Acknowledgements A special thanks to Emmanuel Moliere, Pierre Colon, Mackenson Louis, CTE-RMPP and UHM staff for field support and provision of historical data, and Maxwell Pierrilus for data collection support.

Funding The authors would like to thank the Inter-American Development Bank, supplemented by Northwater International, and the Government of Haiti for the financial and logistical support in executing these studies and in publishing the results. In the spirit of making water research in emerging nations openly available, the open access availability of this report was made possible through financial support from HydroLOGICA.

Declarations

Conflict of interest On behalf of all authors, the corresponding author states that there is no conflict of interest.

References

Adamson JK, Jean-Baptiste G, Miner WJ (2016) Summary of groundwater resources in Haiti. In: Wessel GR, Greenberg JK (eds) Geoscience for the public good and global development: toward a sustainable future. Geol Soc Am Spec Pap 520, pp 1–22. https://doi.org/10.1130/2016.2520(14)

Adamson J, LaVanchy T, Stone B, Clark J, Dykstra S, Taylor M (2021) Geological and hydrogeological assessment of the Brito Formation: Municipio de Tola, Nicaragua. Hydrogeol J 29:2285–2304. https://doi.org/10.1007/s10040-021-02360-w

Adamson JK, Miner WJ, Rochat P-Y, Moliere E, Piasecki M, LaVanchy GT, Perez-Monforte S, Rodriquez-Vera M (2022) Significance of river infiltration to the Port-au-Prince metropolitan region: a case study of two alluvial aquifers in Haiti. Hydrogeol J. https://doi.org/10.1007/s10040-022-02491-8

Agbar (2013) Travaux prioritaires de renforcement de la production d'eau: RMPP [Priority works to strengthen water production: RMPP]. Technical report, Interamerican Development Bank and La Agencia Española de Cooperación Internacional para el Desarrollo (AECID), Madrid

Amiel RB, Grodek T, Frumkin A (2010) Characterization of the hydrogeology of the sacred Gihon Spring, Jerusalem: a deteriorating urban karst spring. Hydrogeol J 18:1465–1479. https://doi.org/10.1007/s10040-010-0600-6

Anderson TA, Bestland EA, Wallis I, Guan HD (2019) Salinity balance and historical flushing quantified in a high-rainfall catchment (Mount Lofty Ranges, South Australia). Hydrogeol J 27:1229–1244. https://doi.org/10.1007/s10040-018-01916-7

Andreo B, Vías J, Durán JJ, Jiménez P, López-Geta JA, Carrasco F (2008) Methodology for groundwater recharge assessment in carbonate aquifers: application to pilot sites in southern Spain. Hydrogeol J 16:911–925. https://doi.org/10.1007/s10040-008-0274-5

Baker A, Berthelin R, Cuthbert M, Treble PC, Hartmann A (2020) Rainfall recharge thresholds in a subtropical climate determined using a regional cave drip water monitoring network. J Hydrol 587:125001. https://doi.org/10.1016/j.jhydrol.2020.125001

Bauer H, Schröckenfuchs TC, Decker K (2016) Hydrogeological properties of fault zones in a karstified carbonate aquifer (Northern Calcareous Alps, Austria). Hydrogeol J 24:1147–1170. https://doi.org/10.1007/s10040-016-1388-9

Bauer-Gottwein P, Gondwe BRN, Charvet G, Marín LE, Rebolledo-Vieyra M, Merediz-Alonso G (2011) Review: The Yucatán Peninsula karst aquifer, Mexico. Hydrogeol J 19:507–524. https://doi.org/10.1007/s10040-010-0699-5

Boisson D, Pubellier M (1987) Carte géologique à 1/250 000 de la République d'Haïti [Geologic map of the Republic of Haiti at 1/250,000] BME, IMAGEO, CNRS, Paris

BRGM [Bureau de Recherches Géologiques et Minières] (1990) Étude des ressources en eau de la région de Port-au-Prince [Study of the water resources of the Port-au-Prince region]. BRGM, Orleans, France

Brunetti E, Jones JP, Petitta M, Rudolph DL (2013) Assessing the impact of large-scale dewatering on fault-controlled aquifer systems: a case study in the Acque Albule basin (Tivoli, central Italy). Hydrogeol J 21:401–423. https://doi.org/10.1007/s10040-012-0918-3

CIAT (Comité Interministériel d'Aménagement du Territoire) (2013) Haiti: Strategic Program for Climate Change Resilience. Bureau du Premier Ministre, République d'Haiti, Port-au-Prince, 181 pp

Clauzon V, Mayolle S, Leonardi V, Brunet P, Soliva R, Marchand P, Massonnat G, Rolando JP (2020) Fault zones in limestones: impact on karstogenesis and groundwater flow (Lez aquifer, southern France). Hydrogeol J 28:2387–2408. https://doi.org/10.1007/s10040-020-02189-9

CNIGS (Centre National de l'Information Géo-Spatiale) (2017) LiDAR elevation dataset at 1.5 m grid spacing. Provided in ArcGIS raster format. CNIGS, Vienna

Corvo F, Minotas J, Delgado J, Arroyave C (2005) Changes in atmospheric corrosion rate caused by chloride ions depending on rain regime. Corrosion Science 47(4):883–892. https://doi.org/10.1016/j.corsci.2004.06.003

Cox B, Bachhuber J, Rathje E, Wood C, Kottke A, Green R, Olson S (2011) Shear wave velocity- and geology-based seismic microzonation of Port-au-Prince, Haiti. Earthq Spectra 27(1_suppl1):67–92. https://doi.org/10.1193/1.3630226

Crosbie RS, Peeters LJM, Herron N, McVicar TR, Herr A (2018) Estimating groundwater recharge and its associated uncertainty: use of regression kriging and the chloride mass balance method. J Hydrol 561:1063–1080. https://doi.org/10.1016/j.jhydrol.2017.08.003

de Vries J, Simmers I (2002) Groundwater recharge: an overview of processes and challenges. Hydrobiol J 10:5–17. https://doi.org/10.1007/s10040-001-0171-7

DGTP [Direction Generale des Travaux Publics] (1918–1938) Bulletin Hydrographique, Les Eaux de Surface de la Republique d'Haiti (Hydrographic Bulletin, Surface water of the Republic of Haiti). DGTP, Port-au-Prince, 16 bulletin reports in the series

Eptisa (2016) Réalisation d'études hydrogéologiques sur la région métropoliaine de Port-au-Prince (RMPP) [Hydrogeologic studies of the metropolitan region of Port-au-Prince]. Geologic map and water point database

FAO [Food and Agriculture Organization of the United Nations] (2010) Haiti: agro ecological zones. Map. FAO, Rome

Fernández-Alvarez JC, Sorí R, Pérez-Alarcón A, Nieto R, Gimeno L (2020) The role of tropical cyclones on the total precipitation in Cuba during the hurricane season from 1980 to 2016. Atmosphere 11:1156. https://doi.org/10.3390/atmos11111156

Fick SE, Hijmans RJ (2017) WorldClim 2: new 1-km spatial resolution climate surfaces for global land areas. Int J Climatol 37(12):4302–4315

Fiorillo F, Leone G, Pagnozzi M, Esposito L (2021) Long-term trends in karst spring discharge and relation to climate factors and changes. Hydrogeol J 29:347–377. https://doi.org/10.1007/s10040-020-02265-0

Ford DC, Williams P (2007) Karst hydrogeology and geomorphology. Wiley, Chichester, UK, 562 pp. https://doi.org/10.1002/9781118684986

Ghasemizadeh R, Yu X, Butscher C, Padilla IY, Alshawabkeh A (2016) Improved regional groundwater flow modeling using drainage features: a case study of the central northern karst aquifer system of Puerto Rico (USA). Hydrogeol J 24:1463–1478. https://doi.org/10.1007/s10040-016-1419-6

Gioda A, Mayol-Bracero OL, Scatena FN, Weathers KC, Mateus VL, McDowell WH (2013) Chemical constituents in clouds and rainwater in the Puerto Rican rainforest: potential sources and seasonal drivers. Atmos Environ 68:208–220. https://doi.org/10.1016/j.atmosenv.2012.11.017.

Goldscheider N (2019) A holistic approach to groundwater protection and ecosystem services in karst terrains. Carbon Evapor 34(4):1241–1249. https://doi.org/10.1007/s13146-019-00492-5

Goldscheider N, Chen Z, Auler AS, Bakalowicz M, Broda S, Drew D, Hartman J, Jiang G, Moosdorf N, Stevanovic Z, Veni G (2020) Global distribution of carbonate rocks and karst water resources. Hydrogeol J 28:1661–1677. https://doi.org/10.1007/s10040-020-02139-5

Gonfiantini R, Simonot M (1988) Isotopic investigation of groundwater in the Cul-de-Sac Plain, Haiti. IAEA-SM-299/132, International Atomic Energy Agency, Vienna, 22 pp

Gourcy L, Adamson JK, Miner WJ, Vitvar T, Belizaire D (2022) The use of water stable isotopes for a better understanding of hydrogeological processes in Haiti: overview of existing δ18O and δ2H data. Hydrogeol J. https://doi.org/10.1007/s10040-022-02498-1

Hartmann A, Liu Y, Olarinoye T et al (2021) Integrating field work and large-scale modeling to improve assessment of karst water resources. Hydrogeol J 29:315–329. https://doi.org/10.1007/s10040-020-02258-z

He Q, Yang P, Yuan W, Jiang Y, Pu J, Yuan D, Kuang Y (2010) The use of nitrate, bacteria and fluorescent tracers to characterize groundwater recharge and contamination in a karst catchment, Chongqing, China. Hydrogeol J 18:1281–1289. https://doi.org/10.1007/s10040-010-0594-0

Huang H, Chen Z, Wang T, Xiang C, Zhang L, Zhou G, Sun B, Wang Y (2019) Nitrate distribution and dynamics as indicators to characterize karst groundwater flow in a mined mineral deposit in southwestern China. Hydrogeol J 27:2077–2089. https://doi.org/10.1007/s10040-019-01987-0

Jebreen H, Wohnlich S, Wisotzky F, Banning A, Hachenberg A, Ghanem M (2018) Recharge estimation in semi-arid karst catchments: Central West Bank, Palestine. Grundwasser 23. https://doi.org/10.1007/s00767-017-0376-x.

Jones I, Banner J (2003) Estimating recharge thresholds in tropical karst island aquifers: Barbados, Puerto Rico and Guam. J Hydrol 278:131–143. https://doi.org/10.1016/S0022-1694(03)00138-0

Kamps RH, Tatum GS, Gault M, Groeger AW (2009) Goodenough Spring, Texas, USA: discharge and water chemistry of a large spring deeply submerged under the binational Amistad Reservoir. Hydrogeol J 17:891–899. https://doi.org/10.1007/s10040-008-0404-0

Kang F, Jin M, Qin P (2011) Sustainable yield of a karst aquifer system: a case study of Jinan springs in northern China. Hydrogeol J 19:851–863. https://doi.org/10.1007/s10040-011-0725-2

Karami GH, Bagheri R, Rahimi F (2016) Determining the groundwater potential recharge zone and karst springs catchment area: Saldoran region, western Iran. Hydrogeol J 24:1981–1992. https://doi.org/10.1007/s10040-016-1458-z

Katz B, Eberts S, Kauffman L (2011) Using Cl/Br ratios and other indicators to assess potential impacts on groundwater quality from septic systems: a review and examples from principal aquifers in the United States. J Hydrol 397:151–166. https://doi.org/10.1016/j.jhydrol.2010.11.017

Kocel E, Stewart R, Mann P, Chang L (2016) Near-surface geophysical investigation of the 2010 Haiti earthquake epicentral area: Léogâne, Haiti. Interpretation 4(1):T49–T61. https://doi.org/10.1190/INT-2015-0038.1

La Vigna F, Mazza R, Amanti M, Di Salvo C, Petitta M, Pizzino L, Pietrosante A, Martarelli L, Bonfà I, Capelli G, Cinti D, Ciotoli F, Ciotoli G, Conte G, Del Bon A, Dimasi M, Falcetti S, Gafà RM, Lacchini A et al (2016) Groundwater of Rome. J Maps 12(Suppl 1):88–93. https://doi.org/10.1080/17445647.2016.1158669

Langston AL, Screaton EJ, Martin JB et al (2012) Interactions of diffuse and focused allogenic recharge in an eogenetic karst aquifer (Florida, USA). Hydrogeol J 20:767–781. https://doi.org/10.1007/s10040-012-0845-3

Long AJ, Sawyer JF, Putnam LD (2008) Environmental tracers as indicators of karst conduits in groundwater in South Dakota, USA. Hydrogeol J 16:263–280. https://doi.org/10.1007/s10040-007-0232-7

Luo M, Chen Z, Zhou H, Zhang L, Han Z (2018) Hydrological response and thermal effect of karst springs linked to aquifer geometry and recharge processes. Hydrogeol J 26:629–639. https://doi.org/10.1007/s10040-017-1664-3

Malík P, Coplák M, Švasta J (2021) Recharge, delayed groundwater-level rise and specific yield in the Triassic karst aquifer of the Kopa Mountain, in the Western Carpathians, Slovakia. Hydrogeol J 29:499–518. https://doi.org/10.1007/s10040-020-02231-w

Marei A, Khayat S, Weise S, Ghannam S, Sbaih M, Geyer S (2010) Estimating groundwater recharge using the chloride mass-balance method in the West Bank, Palestine. Hydrol Sci J 55(5):780–791

Matheswaran K, Khadka A, Dhaubanjar S, Bharati L, Kumar S, Shrestha S (2019) Delineation of spring recharge zones using environmental isotopes to support climate-resilient interventions in two mountainous catchments in Far-Western Nepal. Hydrogeol J 27:2181–2197. https://doi.org/10.1007/s10040-019-01973-6

Mayer A, May W, Lukkarila C, Diehl J (2007) Estimation of fault-zone conductance by calibration of a regional groundwater flow model: Desert Hot Springs, California. Hydrogeol J 15:1093–1106. https://doi.org/10.1007/s10040-007-0158-0

MDE [Ministere de L'Environnement] (2001) Haiti national report: integrating the management of watersheds and coastal areas in Haiti. Unite de Mise en Oeuvre du Plan D'Action Pour L'Environnement (UMO-PAE), Port-au-Prince

Moknatian M, Piasecki M (2021) Development of predictive models for water budget simulations of closed-basin lakes: case studies of Lakes Azuei and Enriquillo on the Island of Hispaniola. Hydrology 8:148. https://doi.org/10.3390/hydrology8040148

Mudarra M, Andreo B, Marín AI, Vadillo I, Barberá JA (2014) Combined use of natural and artificial tracers to determine the hydrogeological functioning of a karst aquifer: the Villanueva del Rosario system (Andalusia, southern Spain). Hydrogeol J 22:1027–1039. https://doi.org/10.1007/s10040-014-1117-1

Nanni T, Vivalda PM, Palpacelli S Marcellini M, Tazioli A (2020) Groundwater circulation and earthquake-related changes in hydrogeological karst environments: a case study of the Sibillini Mountains (central Italy) involving artificial tracers. Hydrogeol J 28:2409–2428. https://doi.org/10.1007/s10040-020-02207-w

Naranjo G, Cruz-Fuentes T, Cabrera M, Custodio E (2015) Estimating natural recharge by means of chloride mass balance in a volcanic aquifer: northeastern Gran Canaria, Canary Islands, Spain. Water 7:2555–2574. https://doi.org/10.3390/7062555

Northwater International and Rezodlo (2018) Hydrogeological characterization of Tunnel Diquini: Port-au-Prince. Technical report, HA-T1239-P001, Inter-American Development Bank, Port-au-Prince, Haiti

Northwater International and Rezodlo (2019) Plaine du cul-de-sac groundwater flow model and model scenarios appendix: Department Ouest. Technical report, Inter-American Development Bank, Port-au-Prince, Haiti, 29 pp

Northwater International and Rezodlo (2020) Hydrogeological characterization of Source Mariani. Technical report, HA-T1239-P001, Inter-American Development Bank, Port-au-Prince, Haiti

Pacheco RL, Bejarano C, Riverón Zaldivar A, Carmenate JA (2004) Composición química de las precipitaciones, deposición de sales y evaluación de la recarga en la región oriental de Cuba [Precipitation chemical composition, salt deposition and recharge assessment in eastern Cuba]. Bol Geol Minero 115:341

Petitta M, Mastrorillo L, Preziosi E, Banzato F, Barberio MD, Billi A, Cambi C, De Luca G, Di Carlo G, Di Curzio D, Di Salvo C, Nanni T, Palpacelli S, Rusi S, Saroli M, Tallini M, Tazioli A, Valigi D, Vivalda P, Doglioni C (2018) Water-table and discharge changes associated with the 2016–2017 seismic sequence in central Italy: hydrogeological data and a conceptual model for fractured carbonate aquifers. Hydrogeol J 26:1009–1026. https://doi.org/10.1007/s10040-017-1717-7

Plan L, Stadler H. (2010) Case study: Kläffer Spring—the major spring of the Vienna Water Supply (Austria). Kresic N, Stevanovic Z (eds) Groundwater hydrology of springs. Butterworth-Heinemann, Oxford, pp 411–427. https://doi.org/10.1016/B978-1-85617-502-9.00020-7

Pubellier M (2000) Plate boundary readjustment in oblique convergence: example of the Neogene of Hispaniola, Greater Antilles. Tectonics 19(4):630–648

Scanlon BR, Healy R, Cook PG (2002) Choosing appropriate techniques for quantifying groundwater recharge. Hydrogeol J 10:18–39

Scholl MA, Murphy SF (2014) Precipitation isotopes link regional climate patterns to water supply in a tropical forest, eastern Puerto Rico. Water Resour Res. https://doi.org/10.1002/2013WR014413

Shamsi A, Karami GH, Hunkeler D, Taheri A (2019) Isotopic and hydrogeochemical evaluation of springs discharging from high-elevation karst aquifers in Lar National Park, northern Iran. Hydrogeol J 27:655–667. https://doi.org/10.1007/s10040-018-1873-4

Smiatek G, Kaspar S, Kunstmann H (2013) Hydrological climate change impact analysis for the Figeh Spring near Damascus, Syria. J Hydrometeorol 14(2):571–593. https://doi.org/10.1175/JHM-D-12-065.1

Stallard RF, Murphy SF (2012) Atmospheric inputs to watersheds of the Luquillo Mountains in eastern Puerto Rico. US Geol Surv Prof Pap 1789-D

Stevanovic Z (2019) Karst waters in potable water supply: a global scale overview. Environ Earth Sci 78(23):662. https://doi.org/10.1007/s12665-019-8670-9

Tian L, Gao Y, Yang G, Schwartz B, Cai B, Ray C, Li Y, Wu H (2021) Isotopic tracers of sources of water for springs from the Edwards Aquifer, Central Texas, USA. Hydrol Res 52(3):787–803. https://doi.org/10.2166/nh.2021.011

Ting CS, Kerh T, Liao CJ (1998) Estimation of groundwater recharge using the chloride mass-balance method, Pingtung Plain, Taiwan. Hydrogeol J 6:282–292. https://doi.org/10.1007/s100400050151

Troester JW, Turvey MD (2004) Water-resources reconnaissance of Île de la Gonâve, Haiti. Hydrogeol J 12:224–236. https://doi.org/10.1007/s10040-003-0309-x

UNDP [United Nations Development Program] (1990) Carte hydrogéologique République d'Haiti [Hydrogeologic map of the Republic of Haiti]. United Nations Development Program, New York, scale 1:250,000, 1 sheet

United Nations, Department of Economic and Social Affairs, Population Division (2019) World population prospects 2019, Online Edition. Rev. 1., UN, New York

Waite H (1960) Reconnaissance investigations of public water supplies of Port au Prince and in 12 villages in the Department du Nord, Haiti. United States Geological Survey, Reston, VA

Woodring WP, Brown JS, Burbank WS (1924) Geology of the Republic of Haiti. Department of Public Works, Port-au-Prince, Haiti

Xanke J, Ender A, Grimmeisen F, Goeppert N, Goldscheider N (2020) Hydrochemical evaluation of water resources and human impacts on an urban karst system, Jordan. Hydrogeol J 28:2173–2186. https://doi.org/10.1007/s10040-020-02174-2

Yehdegho B, Reichl P (2002) Recharge areas and hydrochemistry of carbonate springs issuing from Semmering Massif, Austria, based on long-term oxygen-18 and hydrochemical data evidence. Hydrogeol J 10:628–642. https://doi.org/10.1007/s10040-002-0228-2